Supplementary Information

for

Co-crystallization with conformation-specific designed ankyrin repeat proteins explains the conformational flexibility of BCL-W

Johannes Schilling[1,3], Jendrik Schöppe[1,3], Evelyn Sauer[2] and Andreas Plückthun[1]

[1] Biochemisches Institut
Universität Zürich
Winterthurerstrasse 190
CH-8057 Zürich, Switzerland

[2] Biozentrum
Universität Basel
Klingelbergstrasse 50/70
CH-4056 Basel, Switzerland

[3] These authors contributed equally to this work

Correspondence should be addressed to
Prof. Andreas Plückthun, Biochemisches Institut, Universität Zürich, Winterthurerstr. 190, CH-8057 Zürich, Switzerland, phone: +41-44-635 5570, plueckthun@bioc.uzh.ch.

```
hsBCL-2   ------------------------------------------------------------------------------
hsBCL-XL  ------------------------------------------------------------------------------
BCL-XL    ------------------------------------------------------------------------------
hsBCL-W   ------------------------------------------------------------------------------
BCL-W     ------------------------------------------------------------------------------
hsMCL-1   MFGLKRNAVIGLNLYCGGAGLGAGSGGATRPGGRLLATEKEASARREIGGGEAGAVIGGSAGASPPSTLTPDSRRVARPP 80
                  10        20        30        40        50        60        70        80

hsBCL-2   ------------------------------------------------------------------------------
hsBCL-XL  ------------------------------------------------------------------------------
BCL-XL    ------------------------------------------------------------------------------
hsBCL-W   ------------------------------------------------------------------------------
BCL-W     ------------------------------------------------------------------------------
hsMCL-1   PIGAEVPDVTATPARLLFFAPTRRAAPLEEMEAPAADAIMSPEEELDGYEPEPLGKRPAVLPLLELVGESGNNTSTDGSL 160
                  90       100       110       120       130       140       150       160
                            α1
hsBCL-2   -------MAHAGRTGYDNREIVMKYIHYKLSQRGYEWDAGDVGAAPPGAAPAPGIFSSQPGHTPHPAASRDPVARTSPLQ 73
hsBCL-XL  -------------MSQSNRELVVDFLSYKLSQKGYSWSQFSDVEENRTEAPEGTESEMETPSAINGNPSWHLADSPAVNG 67
BCL-XL    -------------MSQSNRELVVDFLSYKLSQKGYSWSQFSDVEENRTEAPEGTESE----------------------
hsBCL-W   --------MATPASAPDTRALVADFVGYKLRQKGYVCG---------------------------------------- 30
BCL-W     ---------ATPASAPDTRALVADFVGYKLRQKGYVCG---------------------------------------
hsMCL-1   PSTPPPAEEEEDELYRQSLEIISRYLREQATGAKDTKPMG-------------------------------------- 200
                 170       180       190       200
                            α2   BH3          α3          α4                BH1 α5
hsBCL-2   TPAAPGAAAGPALSPVPPVVHLALRQAGDDFSRRYRGDFAEMSSQLHLTPFTARGRFATVVEELFRDGV-NWGRIVAFFE 152
hsBCL-XL  ATAHSSSLDAREVIPMA-AVKQALREAGDEFELRYRRAFSDLTSQLHITPGTAYQSFEQVVNELFRDGV-NWGRIVAFFS 145
BCL-XL    ------------------AVKQALREAGDEFELRYRRAFSDLTSQLHITPGTAYQSFEQVVNELFRDGV-NWGRIVAFFS
hsBCL-W   --------AGPGEGPAADPLHQAMRAAGDEFETRFRRTFSDLAAQLHVTPGSAQQRFTQVSDELFQGGP-NWGRLVAFFV 101
BCL-W     --------AGPGEGPAADPLHQAMRAAGDEFETRFRRTFSDLAAQLHVTPGSAQQRFTQVSDELFQGGP-NWGRLVAFFV
hsMCL-1   -----------RSGATSRKALETLRRVGDGVQRNHETAFQGMLRKLDIKNEDDVKSLSRVMIHVFSDGVTNWGRIVTLIS 269
                           210       220       230       240       250       260
                   α6                α7   BH2 α8      α9
hsBCL-2   FGGVMCVESVNREMSPLVDNIALWMTEYLNRHLHTWIQDNGGWDAFVELYGPSMRPLFDFSWLSLKTLLSLALVGACITL 232
hsBCL-XL  FGGALCVESVDKEMQVLVSRIAAWMATYLNDHLEPWIQENGGWDTFVELYGNNAAAESRKGQERFNRWFLTGMTVAGVVL 225
BCL-XL    FGGALCVESVDKEMQVLVSRIAAWMATYLNDHLEPWIQENGGWDTFVELYG-----------------------------
hsBCL-W   FGAALCAESVNKEMEPLVGQVQEWMVAYLETRLADWIHSSGGWAEFTALYGDGALEEARRLREGNWASVRTVLTGAVALG 181
BCL-W     FGAALCAESVNKEMEVLVGQVQEWMVAYLETRLADWIHSSGGWAEFTALYGDGALEEARRLREGNWASVR----------
hsMCL-1   FGAFVAKHLKTINQESCIEPLAESITDVLVRTKRDWLVKQRGWDGFVEFFHVEDLEGGIRNVLLAFAGVAGVGAGLAYLI 349
                  280       290       300       310       320       330       340

hsBCL-2   GAYLSHK                                                                          239
hsBCL-XL  LGSLFSRK                                                                         233
BCL-XL    --------
hsBCL-W   ALVTVGAFFASK                                                                     193
BCL-W     ------------
hsMCL-1   R                                                                                350
```

Suppl. Figure S1. Structure-based sequence alignment of the human variants (*homo sapiens*, hs) of anti-apoptotic BCL-2 family members BCL-2, BCL-XL, BCL-W and MCL-1. Sequences of BCL-XL as used in the truncated 1MAZ structure and the sequence of our crystallized BCL-W construct (both denoted without hs) are included in the alignment and are listed below the sequence of the full-length human variants. The BH domains are indicated by colored bars above the sequence and helix regions as colored bars on the sequence. The displaceable groove-binding helix α9 of BCL-W is highlighted in yellow. Boxes indicate hinge regions and residues interacting with the hinge regions (α2-α3 hinge (blue) and α4-α5 hinge (red)).

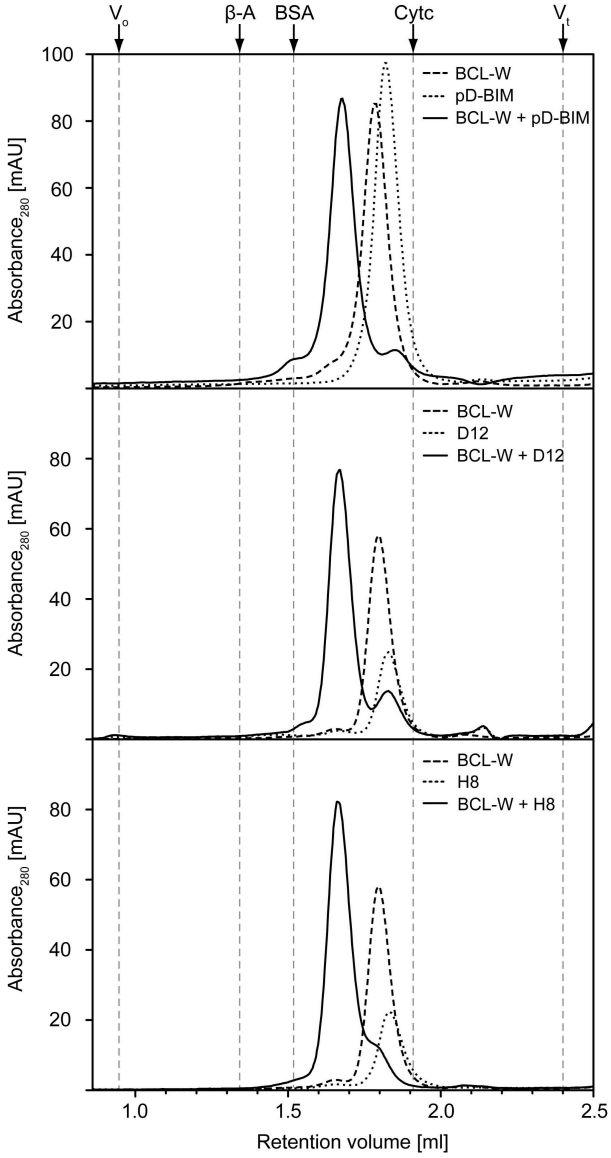

Suppl. Figure S2. Complex formation of BCL-W ($MW_{theor.}$ 22 kDa) with ligands (either pD-BIM ($MW_{theor.}$ 16 kDa), DARPin D12 ($MW_{theor.}$ 18 kDa) or DARPin H8 ($MW_{theor.}$ 18 kDa)). Superposition of analytical SEC elution profiles of BCL-W, ligands and complexes thereof are shown. Free BCL-W (dashed line), free ligand (short dashed line) and BCL-W complexed with the ligand (solid line) are shown. Protein elution was followed by UV absorption at 280 nm. Free BCL-W and ligands (pD-BIM, D12 or H8) as well as equimolar complexes thereof were used at a concentration of 10 μM. Upon ligand binding a clear shift of the complex peak (solid line) to a higher molecular weight (smaller retention volume) can be observed. In all three cases, minor tailing shoulders at higher retention volumes are present in the complex elution profile. These shoulders can be attributed to either uncomplexed BCL-W or uncomplexed ligand. The void volume (V_o = 0.95 ml), the total volume (V_t = 2.4 ml) and the molecular mass standards (β-amylase with an apparent mass of 200 kDa, BSA with an apparent mass of 66 kDa and cytochrome c with an apparent mass of 12.4 kDa) are indicated by broken gray lines in the graph.

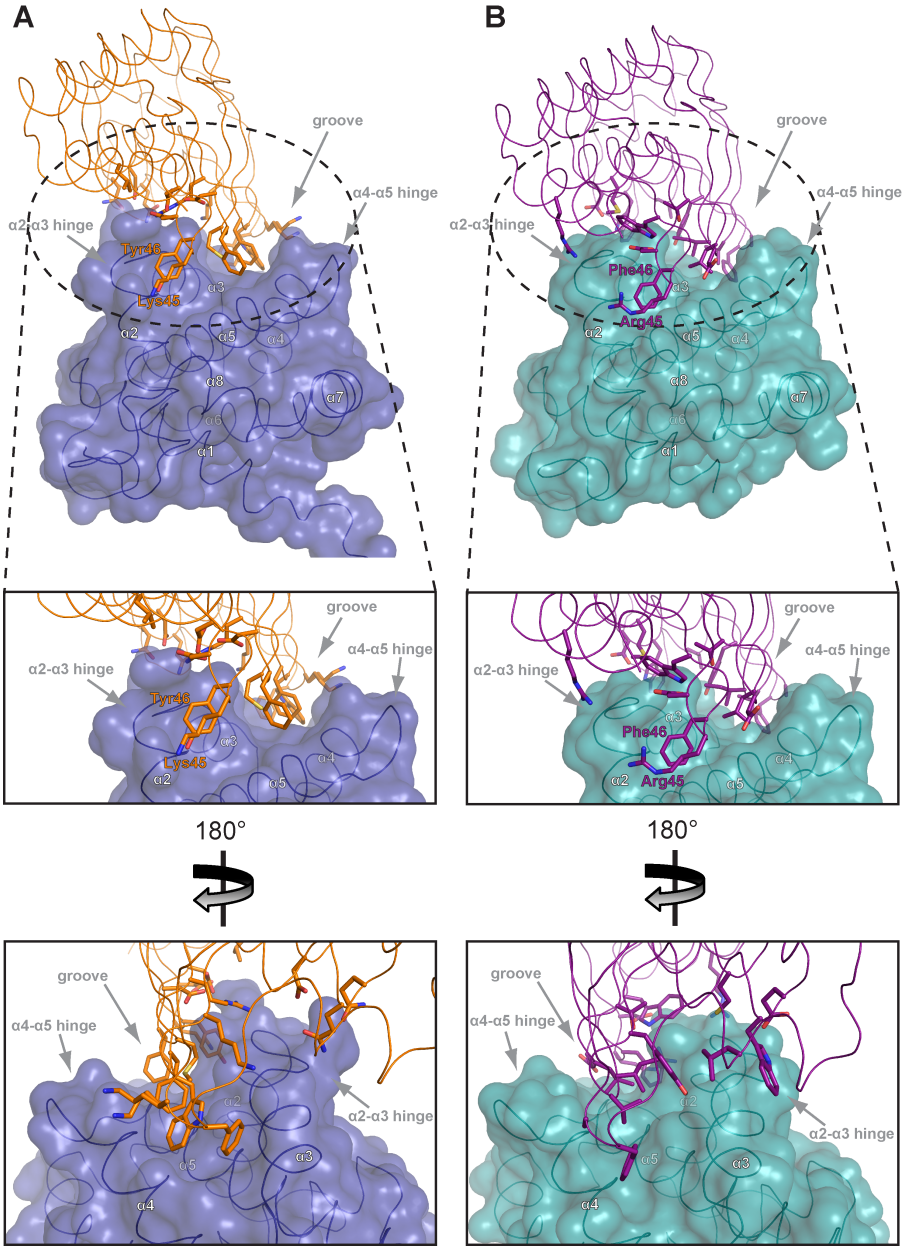

Suppl. Figure S3. Binding of DARPins to the BCL-W groove. BCL-W is shown as a transparent, molecular surface with a ribbon representation of the protein backbone in blue and cyan, respectively. The corresponding DARPins D12 and H8 are shown in orange and purple in a ribbon diagram with interacting positions highlighted as sticks. (A) View along the BCL-W groove in the BCL-W/D12 complex. The close-up from the same perspective and a 180° turned view show mainly bulky, aromatic residues which are buried inside the hydrophobic pocket. The interacting positions of the helical positions and the β-turn stems on the DARPin consist of polar and charged side-chains that provide contacts to residues protruding from the adjacent α-helix of BCL-W. (B) View along the BCL-W groove in the BCL-W/H8 complex. The main difference to the BCL-W/D12 complex lies in the presence of shorter hydrophobic residues at the randomized β-turn positions allowing a deeper penetration into the binding groove.

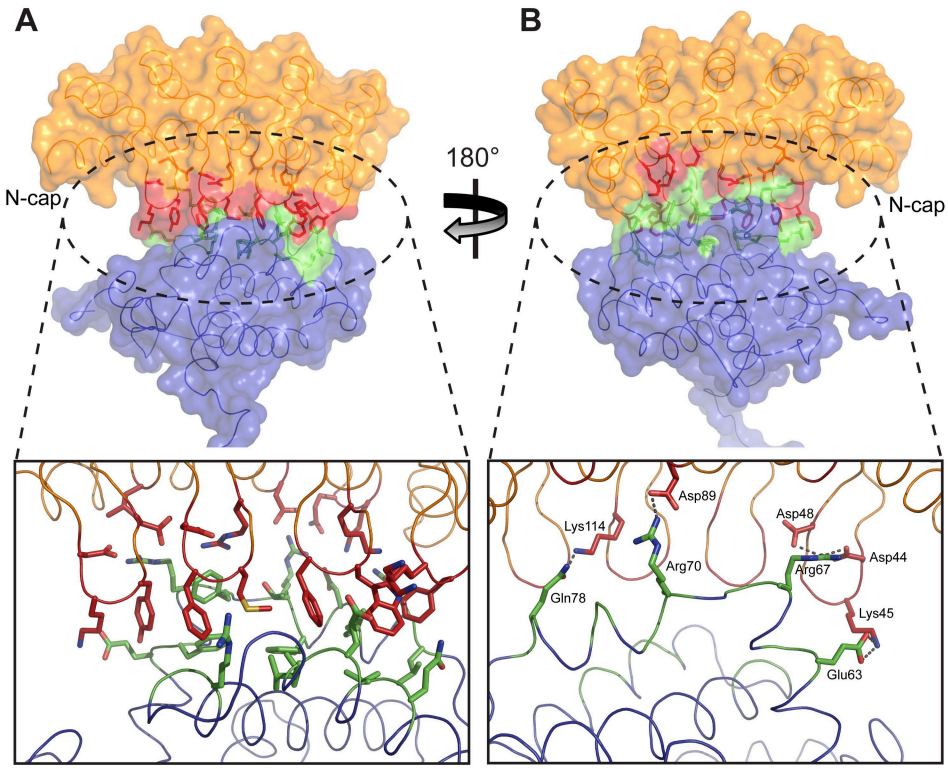

Suppl. Figure S4. Visualization of interface residues of BCL-W and DARPin D12. In (A) and (B), the complex between BCL-W (blue) and D12 (orange) is shown from the front and the back as a transparent molecular surface with a ribbon representation of the protein backbones. The surface of interface residues is colored green (BCL-W) and red (D12), respectively. Interface residues within a distance of 4 Å are highlighted. The close-ups of marked regions allow the assessment of interacting residues (stick representation) in more detail. Note that in the close-up of (A), all interacting residues are shown, whereas in the close-up of (B), only residues involved in polar interactions (indicated by black dashed lines) are depicted.

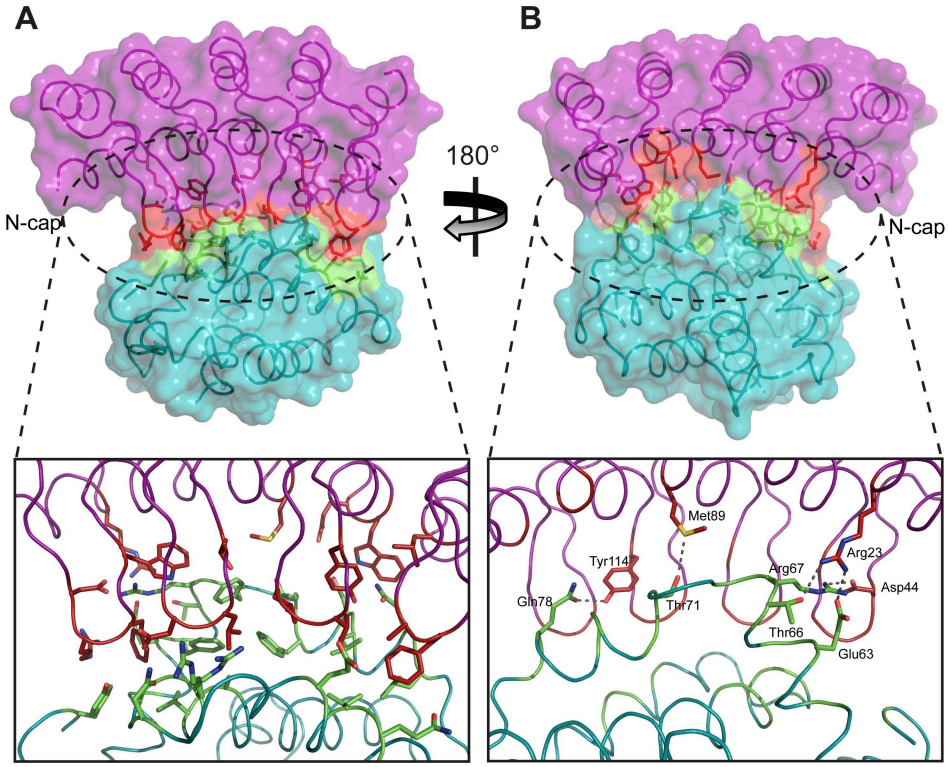

Suppl. Figure S5. Visualization of interface residues of BCL-W and DARPin H8 (first complex in asymmetric unit). In (A) and (B), the complex between BCL-W (cyan) and H8 (purple) is shown from the front and the back as a transparent molecular surface with a ribbon representation of the protein backbones. The surface of interface residues is colored green (BCL-W) and red (H8), respectively. Interface residues within a distance of 4 Å are highlighted. The close-ups of marked regions allow the assessment of interacting residues (stick representation) in more detail. Note that in the close-up of (A), all interacting residues are shown, whereas in the close-up of (B), only residues involved in polar interactions (indicated by black dashed lines) are depicted.

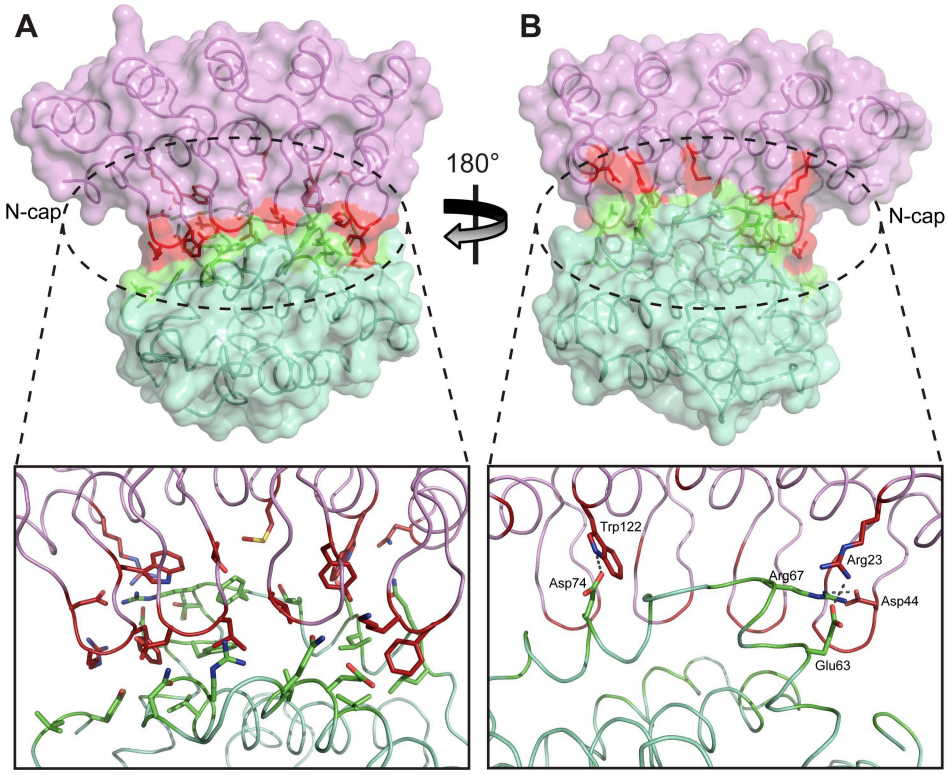

Suppl. Figure S6. Visualization of interface residues of BCL-W and DARPin H8 (second complex in asymmetric unit). In (A) and (B), the complex between BCL-W (light green) and H8 (violet) is shown from the front and the back as a transparent molecular surface with a ribbon representation of the protein backbones. The surface of interface residues is colored green (BCL-W) and red (H8), respectively. Interface residues within a distance of 4 Å are highlighted. The close-ups of marked regions allow the assessment of interacting residues (stick representation) in more detail. Note that in the close-up of (A), all interacting residues are shown, whereas in the close-up of (B), only residues involved in polar interactions (indicated by black dashed lines) are depicted.

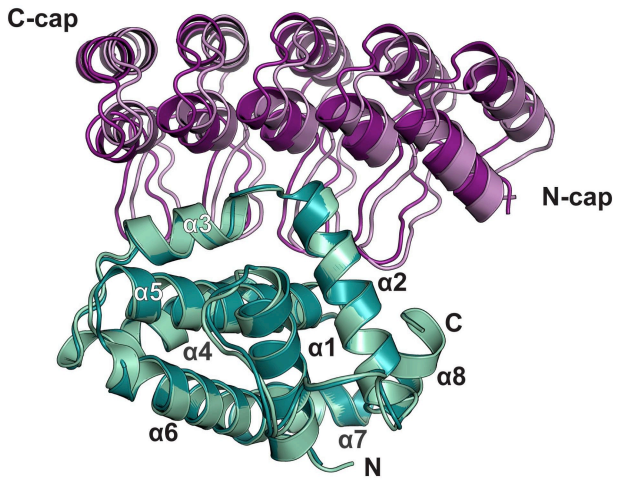

Suppl. Figure S7. Superposition of the two complexes in the asymmetric unit of the BCL-W/H8 structure. DARPin H8 is slightly shifted towards the entrance of the hydrophobic BCL-W groove in the second complex (BCL-W, light green; H8, violet) of the asymmetric unit compared to the first complex (BCL-W, cyan; H8, purple) in the asymmetric unit.

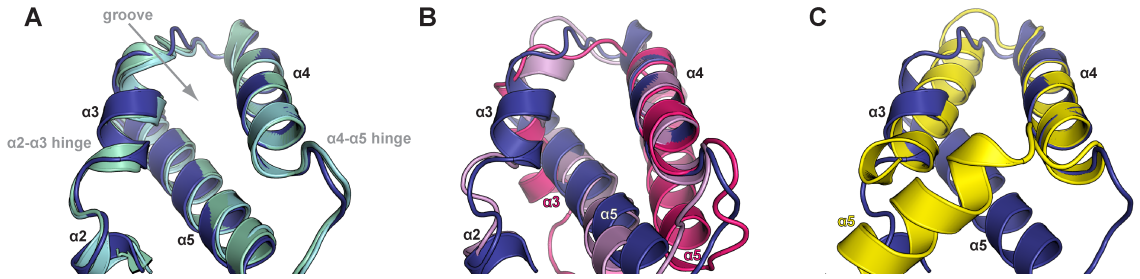

Suppl. Figure S8. Comparison of all available BCL-W surface groove structures through structural alignment of their α4 helix. Structures are shown in ribbon representation. We wanted to elucidate how the new structures in their compact, ligand binding-competent conformation differed from the previous structures of BCL-W, first focusing on the hinge and groove regions. To achieve this, all available BCL-W structures were compared through structural alignment of their α4 helix. (A) First, we compared our new crystal structures of BCL-W to each other. In total, we solved three BCL-W structures: the BCL-W/D12 complex structure BCL-W_{D12} (blue) and two BCL-W/H8 complex structures present in the asymmetric unit of crystals from the BCL-W/H8 complex (cyan and light green) (see Suppl. Table ST3 and Suppl. Figures S5, S6, and S7). Despite the slight differences in DARPin interactions, the structure of BCL-W in both BCL-W/H8 complexes is practically identical, with an overall RMSD including side chains of 0.304 Å. The BCL-W structures from the BCL-W/D12 and BCL-W/H8 complex are still very close, with an overall RMSD including side chains of 0.477 Å for the first BCL-W/H8 complex and 0.419 Å for the second. The BCL-W groove region formed by the α2-α3 hinge, helices α3 and α4, the α4-α5 hinge and helix α5 are practically identical in all of our BCL-W crystal structures, illustrating that the binding of DARPins used for co-crystallization does not alter the intrinsic structure of BCL-W. Since the BCL-W structure in the BCL-W/D12 complex, from now on denoted BCL-W_{D12}, was solved at the highest resolution of 1.5 Å (cf. 1.85 Å resolution for the BCL-W/H8 structure), the BCL-W_{D12} structure was used for comparison to all other available BCL-W structures.

(B) Comparison of BCL-W_{D12} (blue) with the available BCL-W NMR structures (PDB-ID: 1MK3 [1] (pink) and PDB-ID: 1O0L [2] (violet)). Although helices α3, α4 and α5 of 1O0L (violet) align comparably well with BCL-W_{D12} (blue), the conformations of both hinge regions deviate significantly from the BCL-W_{D12} structure. The conformation of the 1MK3 groove deviates considerably from the groove of BCL-W_{D12} and the second NMR structure 1O0L, and neither hinge regions nor helices α3 and α5 of 1MK3 (pink) align with any of the other BCL-W structures.

(C) The only other available BCL-W structure is the domain-swapped BCL-W (BCL-WΔC29; PDB-ID: 2Y6W) [3] crystal structure, showing a large displacement of the groove formed by α3-α4. Comparison of the BCL-W_{D12} (blue) groove to the domain-swapped 2Y6W structure (yellow) shows that, as a result of the domain swap seen in 2Y6W, the conformations of the hinge regions in BCL-W_{D12} and 2Y6W are completely different. Helix α3 in 2Y6W is longer than in BCL-W_{D12}, thereby changing the shape of the groove.

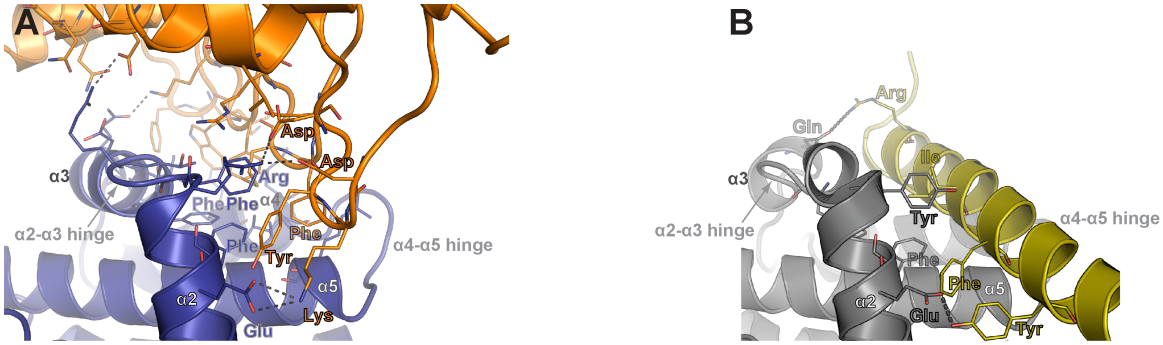

Suppl. Figure S9. Similarities between the interaction network of the DARPin D12/BCL-W_{D12} and the previously reported BIM/BCL-XL complex crystal structure (PDB ID: 1PQ1). (A) Interactions of DARPin D12 (orange) with BCL-W_{D12} (blue). (B) Similar interactions of BIM (olive) with BCL-XL (gray) (PDB ID: 1PQ1). Structures are shown in ribbon representation with interacting residues depicted as sticks. Hydrogen bonds are indicated by black dashed lines.

Tables

Suppl. Table ST1. Statistics for data collection and refinement.

Complex	Statistics
BCL-W/D12	
Data collection	
Space group	mC: C2
Cell dimensions, Å	a = 110.7, b = 42.6, c = 76.7
	a = 90°, b = 110.8°, g = 90°
AU content	1 complex
VM, $Å^3$/Da	2.11
Resolution limits, Å	50 – 1.5
Observed reflections	Total 185703, unique 52907, possible 53934
Completeness, %	98.1 (96.1)*
R-merge, %	5.0 (33.3)*
I/s	14.65 (3.56)*
Refinement	
Resolution range, Å	39.4-1.5
Final R-cryst, R-free, %	14.90, 18.51
Number of residues	325
Number of solvent molecules	402
Number of atoms	2927
Mean B-factor, $Å^2$	19.7
rmsd (bonds), Å	0.005
rmsd (angles), °	0.937
Ramachandran analysis, %	98.8/1.2/0
BCL-W/H8	
Data collection	
Space group	mP: $P2_1$
Cell dimensions, Å	a = 49.3, b = 93.6, c = 72.3
	a = 90°, b = 106.8°, g = 90°
AU content	2 complexes
VM, $Å^3$/Da	2.09
Resolution limits, Å	50 – 1.85
Observed reflections	Total 151416, unique 52593, possible 53659
Completeness, %	98.0 (99.1)*
R-merge, %	4.8 (56.0)*
I/s	14.92 (2.11)*
Refinement	
Resolution range, Å	38.7-1.85
Final R-cryst, R-free, %	17.57, 22.21
Number of residues	601
Number of solvent molecules	413
Number of atoms	4931
Mean B-factor, $Å^2$	24.65
rmsd (bonds), Å	0.007
rmsd (angles), °	1.187
Ramachandran analysis, %	98.7/1.0/0.3

* Values in parentheses refer to the highest-resolution shell.

Suppl. Table ST2. List of the major interaction contacts in the BCL-W/D12 complex within a cutoff of 4 Å.

D12 interaction residue (repeat module)*			Chain	H-bond (Å)	BCL-W interaction residue*		Chain
ASP	44	(1)	B	OD2-NH1 (2.76)	ARG	67	A
LYS	45†	(1)	B	NZ-OE1 (3.08)	GLU	63	A
LYS	45†	(1)	B	NZ-OE2 (3.11)	GLU	63	A
TYR	46†	(1)	B		PHE	68	A
TYR	46†	(1)	B		ARG	67	A
TYR	46†	(1)	B		PHE	64	A
TYR	46†	(1)	B		GLU	63	A
ASP	48†	(1)	B	OD2-NH1 (2.92)	ARG	67	A
LEU	53	(1)	B		ARG	67	A
ASP	77	(2)	B		PHE	68	A
PHE	78†	(2)	B		PHE	64	A
PHE	78†	(2)	B		GLY	105	A
PHE	78†	(2)	B		ARG	106	A
MET	79†	(2)	B		PHE	68	A
MET	79†	(2)	B		PHE	64	A
MET	79†	(2)	B		THR	71	A
MET	79†	(2)	B		PHE	72	A
ARG	81†	(2)	B		PHE	68	A
ARG	81†	(2)	B	NH1-O (3.19)	ARG	67	A
ASP	89†	(2)	B	OD1-NH2 (3.15)	ARG	70	A
PHE	111†	(3)	B		LEU	97*	A
PHE	111†	(3)	B		GLU	96	A
PHE	111†	(3)	B		LEU	75	A
TRP	112†	(3)	B		LEU	75	A
TRP	112†	(3)	B		GLU	96	A
TRP	112†	(3)	B		VAL	93	A
TRP	112†	(3)	B		GLN	92	A
LYS	114†	(3)	B	NZ-OE1 (2.74)	GLN	78	A
GLN	122†	(3)	B		ASP	74	A
GLN	122†	(3)	B		GLN	78	A
GLN	122†	(3)	B		ARG	70	A
GLN	123†	(3)	B		ARG	70	A
LYS	144*	(C-cap)	B		GLU	96	A
PHE	145	(C-cap)	B		GLN	78	A
PHE	145	(C-cap)	B		LEU	79	A
PHE	145	(C-cap)	B		LEU	75	A

†Amino acids are located in a randomized position of D12.
*Amino acids are present in alternative conformations.

Suppl. Table ST3. List of the major interaction contacts in the BCL-W/H8 complex.

H8 interaction residue (repeat module)*			Chain	H-bond (Å)	BCL-W interaction residue*		Chain
ARG	23	(N-cap)	A		ARG	67	D
ARG	23	(N-cap)	A	NH1-OE2 (2.59)	GLU	63	D
ARG	23	(N-cap)	A	NH2-OG1 (353)	THR	66	D
ASP	44	(1)	A	OD2-NH1 (2.67)	ARG	67	D
ARG	45†	(1)	A	O-OH (2.6)	TYR	162	D
ARG	45†	(1)	A		GLU	63	D
PHE	46†	(1)	A		PHE	64	D
PHE	46†	(1)	A		ARG	67	D
PHE	46†	(1)	A		VAL	108	D
PHE	46†	(1)	A		TYR	162	D
PHE	46†	(1)	A		GLU	63	D
PHE	46†	(1)	A		ALA	60	D
TRP	48†	(1)	A		ARG	67	D
TRP	48†	(1)	A		PHE	68	D
ASP	78†	(2)	A		ARG	106*	D
ASP	78†	(2)	A		ASN	103	D
ASP	78†	(2)	A		GLY	105	D
LEU	79†	(2)	A		ALA	109	D
LEU	79†	(2)	A		PHE	72	D
LEU	79†	(2)	A		PHE	64	D
LEU	79†	(2)	A		ARG	106*	D
THR	81†	(2)	A		PHE	68	D
MET	89‡	(2)	A	SD-OG1 (3.59)	THR	71	D
ILE	111†	(3)	A		THR	71	D
ILE	111†	(3)	A		PHE	68	D
VAL	112†	(3)	A		GLU	96	D
VAL	112†	(3)	A		LEU	75	D
TYR	114†	(3)	A	OH-OE1 (2.6)	GLN	78	D
TYR	114†	(3)	A		LEU	75	D
TRP	122†	(3)	A		ASP	74	D
TRP	122†	(3)	A		GLN	78	D
GLU	123†	(3)	A		ASP	74	D
LYS	144	(C-cap)	A		GLU	96	D
PHE	145	(C-cap)	A		GLN	92	D
PHE	145	(C-cap)	A		LEU	79	D
PHE	145	(C-cap)	A		VAL	93	D
LEU	152	(C-cap)	A		GLN	78	D
ARG	23	(N-cap)	B	NH1-OE2 (2.66)	GLU	63	C
ARG	23	(N-cap)	B		THR	66*	C
ASP	44	(1)	B	OD1-NH1 (2.93)	ARG	67	C
ARG	45†	(1)	B	O-OH (2.45)	TYR	162	C
ARG	45†	(1)	B		GLU	63	C
ARG	45†	(1)	B		LEU	161	C
PHE	46†	(1)	B		PHE	64	C
PHE	46†	(1)	B		ARG	67	C
PHE	46†	(1)	B		VAL	108	C
PHE	46†	(1)	B		TYR	162	C
PHE	46†	(1)	B		GLU	63	C
PHE	46†	(1)	B		ALA	60	C
TRP	48†	(1)	B		ARG	67	C
TRP	48†	(1)	B		PHE	68	C
ASP	78†	(2)	B		ARG	106	C
ASP	78†	(2)	B		ASN	103	C
ASP	78†	(2)	B	OD2-N (3.23)	GLY	105	C
LEU	79†	(2)	B		GLY	105	C
LEU	79†	(2)	B		LEU	97	C
THR	81†	(2)	B		PHE	68	C
MET	89†	(2)	B		ARG	67	C
ILE	111†	(3)	B		THR	71	C
ILE	111†	(3)	B		PHE	68	C
ILE	111†	(3)	B		GLU	96	C
TYR	114†	(3)	B		LEU	75	C
TRP	122†	(3)	B	NE1-OD2 (3.02)	ASP	74	C
TRP	122†	(3)	B		THR	71	C
LYS	144	(C-cap)	B		GLU	96	C
LYS	144	(C-cap)	B		GLN	99	C
PHE	145	(C-cap)	B		LEU	79	C
PHE	145	(C-cap)	B		VAL	93	C
ASN	156	(C-cap)	B		GLN	78	C

*A cutoff of 4 Å was applied for interactions.

† Amino acids are located in a randomized position of H8.

References

1. Denisov, A.Y., Madiraju, M.S.R., Chen, G., Khadir, A., Beauparlant, P., Attardo, G., Shore, G.C. & Gehring, K. (2003). Solution structure of human BCL-w: modulation of ligand binding by the C-terminal helix. *J. Biol. Chem.* **278**, 21124–21128
2. Hinds, M.G., Lackmann, M., Skea, G.L., Harrison, P.J., Huang, D.C.S. & Day, C.L. (2003). The structure of Bcl-w reveals a role for the C-terminal residues in modulating biological activity. *EMBO J* **22**, 1497–1507
3. Lee, E.F., Dewson, G., Smith, B.J., Evangelista, M., Pettikiriarachchi, A., Dogovski, C., Perugini, M.A., Colman, P.M. & Fairlie, W.D. (2011). Crystal structure of a BCL-W domain-swapped dimer: implications for the function of BCL-2 family proteins. *Structure* **19**, 1467–1476